

## Supplementary Material

### Structural foundations for the O<sub>2</sub> resistance of *Desulfomicrobium baculatum* [NiFeSe]-hydrogenase

Anne Volbeda,<sup>\*a</sup> Patricia Amara,<sup>a</sup> Marina Iannello,<sup>a</sup> Antonio L. De Lacey,<sup>b</sup> Christine Cavazza<sup>a</sup> and Juan Carlos Fontecilla-Camps<sup>a</sup>

<sup>a</sup> Metalloproteins Unit, Institut de Biologie Structurale J.P. Ebel, CEA, CNRS, Université Grenoble Alpes UMR 5075, 41 rue Jules Horowitz, 38027 Grenoble, France.

<sup>b</sup> Instituto de Catálisis y Petroleoquímica, CSIC, c/Marie Curie 2, 28049 Madrid, Spain.

**Enzyme purification.** *Desulfomicrobium baculatum* (*Dmb*) cells (260 g) were suspended in 10 mM Tris/HCl pH 7.6 (Buffer A), 10 µg/mL DNase I and a complete protease inhibitor cocktail (Roche) and broken in a microfluidizer. Cell debris was removed by centrifugation at 15000 g for 45 min, after which the supernatant was centrifuged at 35000 rpm for 1h30. Two independent enzyme purifications were performed using the same protocol at room temperature, the first one (prep-I) under air and the second one (prep-II) under anaerobic conditions in a glove box (Jacomex, France). The supernatant obtained from the broken cell suspension was loaded on a DEAE cellulose column, which like all subsequent columns was first equilibrated with buffer A. The non-retained fraction containing hydrogenase was loaded on a Q-Sepharose Fats Flow (GE Healthcare UK) column. The absorbed proteins were eluted by applying a linear gradient of NaCl (0→1M) in buffer A. The fraction containing hydrogenase activity eluted at 600 mM NaCl and was concentrated by an Amicon cell (Millipore 30 NMWL). The sample was next applied to a Superdex 200 column and eluted with buffer A + 150 mM NaCl, followed by further purification over a hydroxyapatite column. Hydrogenase activity eluted at 100 mM potassium phosphate (KP) when applying a linear gradient of 1→200 mM KP, using the same buffer. The sample was finally dialyzed against buffer A to remove excess phosphate. Enzyme purity was checked using polyacrylamide gel electrophoresis (PAGE) and electrospray mass spectrometry. Specific hydrogen uptake activity was determined spectrophotometrically at 604 nm by following the color change of oxidized methyl viologen (MV) in a hydrogen-saturated solution, after adding a small amount of enzyme.

**FTIR characterization.** A Nicolet Magna 860 Fourier transform spectrometer equipped with a mercury cadmium telluride detector and an 82- $\mu\text{m}$  path-length transmission cell with  $\text{CaF}_2$  windows was used to record IR spectra of prep-I and prep-II. Both gave similar IR bands, suggesting that the latter was exposed to air during transport. We therefore show only the result for prep-I (Fig. S1A). The spectrum displays three CO bands of comparable intensity at 1941, 1945 and 1955  $\text{cm}^{-1}$ , along with at least six  $\text{CN}^-$  bands between 2061 and 2104  $\text{cm}^{-1}$ . Accordingly, the NiFeSe site is present as a mixture of at least three states. Upon exposure of the same sample to 1 atm of  $\text{H}_2$  during 15 minutes (not shown), the spectrum completely changed and new bands typical for a fully reduced Ni-R state appeared, indicating that all the states present in the as-prep enzyme can be fully activated. The aerobically purified soluble [NiFeSe]-hydrogenase of *Desulfovibrio vulgaris* Hildenborough (*Dvh*) used for crystallization showed a very different FTIR spectrum,<sup>1</sup> with a strong CO band at 1904  $\text{cm}^{-1}$ , a weak one at 1939  $\text{cm}^{-1}$  and three  $\text{CN}^-$  bands between 2079 and 2094  $\text{cm}^{-1}$  (Fig. S1B). These results clearly indicate that the major state observed for the *Dvh* enzyme is not present in the *Dmb* preparations used in the present study, as these showed no 1904  $\text{cm}^{-1}$  band (Fig. S1A).

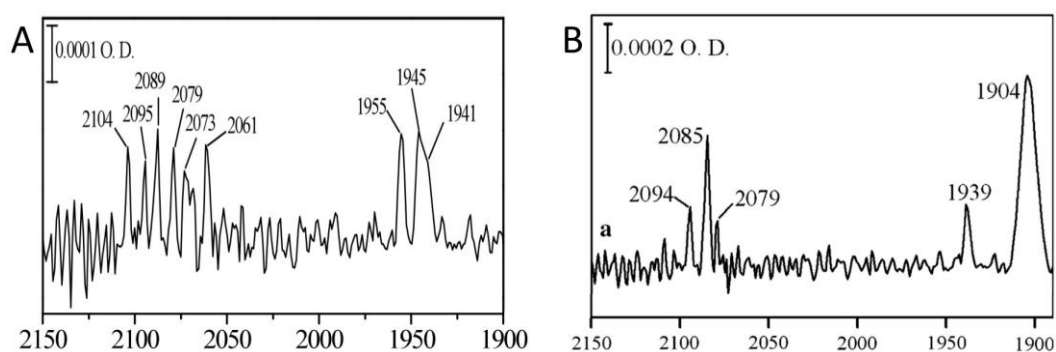


**Figure S1.** FTIR spectra of aerobically purified [NiFeSe]-hydrogenase preparations used for structural studies: **A** Sample in 10 mM Tris/HCl, pH 6.0, from *Desulfomicrobium baculatum*; **B** Enzyme from *Desulfovibrio vulgaris* Hildenborough (from Marques et al.,<sup>1</sup> with permission). Spectral resolution was 2  $\text{cm}^{-1}$  and the baseline was corrected using OMNIC software from Nicolet.

**Crystallization.** After concentration of the purified hydrogenase in an Amicon cell (Millipore 30 NMWL) to 7 mg/mL, crystals were obtained at 4°C under air with the hanging drop vapour diffusion method. Preliminary crystallization trials using prep-I were performed using Peg suite II (Qiagen kit). One  $\mu\text{L}$  of protein solution was mixed with one  $\mu\text{L}$  of reservoir solution and equilibrated against 1 mL of reservoir solution. The most promising conditions

were optimized to give reservoir solutions containing 22 to 27% (W/V) polyethylene glycol (PEG) 4000, 0.1 M Tris/HCl buffer pH 8.5 and 0.2 M CaCl<sub>2</sub>. Crystals appeared after a few days. The crystals obtained with the anaerobic purification (prep-II) diffracted to much higher resolution. A part of prep-II was also used for enzyme activation under H<sub>2</sub> for 1h in the glove box, before starting crystallization at 4°C under air.

**Table S1.** X-ray data statistics.

Data set	<i>N1</i>	<i>N2</i>	<i>N3</i>	<i>N3'</i>	<i>A1</i>	<i>A2a</i>	<i>A2b</i>
Beamline	BM30a	ID14-4	BM30a	BM30a	ID23-1	ID14-4	BM30a
$\lambda$ (Å)	0.9780	1.1399	1.7394	1.7443	0.9465	1.1399	0.9500
Overall resolution (Å)	30-1.52	30-1.70	30-2.00	30-2.00	30-1.40	30-1.60	30.0-1.55
unique reflections	226689	171915	105522	104787	282740	193492	206663
R <sub>sym</sub> (%)	5.7	17.7	8.7	9.6	7.2	15.7	6.2
$\langle I/\sigma_I \rangle$	11.3	6.3	8.7	7.3	8.3	8.0	10.7
completeness (%)	93.7	98.5	98.5	97.8	91.5	93.1	90.5
High-resolution shell (Å)	1.6-1.52	1.8-1.7	2.12-2.0	2.12-2.0	1.48-1.4	1.7-1.6	1.64-1.55
unique reflections	22885	25474	15594	14983	28469	22791	21548
R <sub>sym</sub> (%)	37.5	134.9	26.0	31.2	99.4	176.3	62.8
CC <sub>1/2</sub> (%)	73.7	21.2	84.4	80.4	31.8	16.1	50.3
$\langle I/\sigma_I \rangle$	2.1	0.7	3.3	2.4	0.9	0.6	1.0
completeness (%)	66.9	94.1	91.9	88.3	60.5	66.6	61.1
R <sub>scale</sub> (%)	11.5	15.5	12.4	13.5	0.0	14.0	11.6
B <sub>Wilson</sub> □ □ Å <sup>2</sup> □	17.3	21.7	18.3	18.8	21.0	22.1	21.1

**X-ray data collection.** Flash-cooled crystals stored in liquid nitrogen were exposed to X-rays under a cold N<sub>2</sub> stream at approximately 100 K at three wavelength tunable beamlines of the European Synchrotron Radiation Facility in Grenoble (ESRF, Table S1), generating a beam of relatively low intensity with a bending magnet (BM30A) and of high intensity with an insertion device (ID14-4 and ID23-1). Accordingly, a much longer exposure time was needed at BM30A in order to obtain high resolution data. The crystal space group was P2<sub>1</sub>2<sub>1</sub>2<sub>1</sub> with cell dimensions a=106.2, b=108.7 and c=136.5 Å. Integration, scaling and merging of X-ray reflection data (Table S1), followed by conversion to unique structure factor amplitudes was done with the XDS package.<sup>2</sup> A relatively low value was chosen for the CC<sub>1/2</sub> correlation criterion for choosing the resolution limits for the data sets obtained with the lowest X-ray exposures, assuming that a correlation coefficient higher than 10% indicates useful data.<sup>3</sup> All the used crystals were highly isomorphous, as indicated by the low R<sub>scale</sub> values (Table S1) obtained after scaling of data sets with the CCP4 program *SCALEIT*.<sup>4</sup>

**Structural analyses.** The crystal structure was solved by molecular replacement with *PHASER*,<sup>5</sup> starting from the known structure of *Dmb* [NiFeSe]-hydrogenase in a reduced state (pdb code 1CC1).<sup>6</sup> Manual model corrections were performed with *COOT*.<sup>7</sup> The *REFMAC* program<sup>8</sup> was used for refinement of atomic positions and individual anisotropic temperature factors ( $B_{\text{aniso}}$ ) for all data sets except *N3b*, where TLS parameters along with positional parameters and isotropic B-factors were refined. Refined models of the highest resolution data sets obtained from the non-activated (*NI*) and activated (*AI*) enzyme preparation were used as starting models for refining the other data sets, after an initial rigid body refinement. In order to increase the signal-to-noise level of the various electron density maps, they were averaged over the two hydrogenase molecules contained in the asymmetric unit with the home-made program *SUPERED*. Unbiased views of the active site were obtained with averaged omit-maps calculated from  $mF_{\text{obs}}-F_{\text{calc}}$  coefficients.<sup>9</sup> Hydrophobic tunnels were calculated with the home-made program *CAVENV*, included in CCP4,<sup>4</sup> and displayed for an accessible probe radius of 1.0 Å (Fig. S2). Furthermore, the programs *MOLSCRIPT*,<sup>10</sup> *CONSCRIPT*<sup>11</sup> and *RASTER3D*<sup>12</sup> were used to generate Figures 1-3 and Fig. 5.

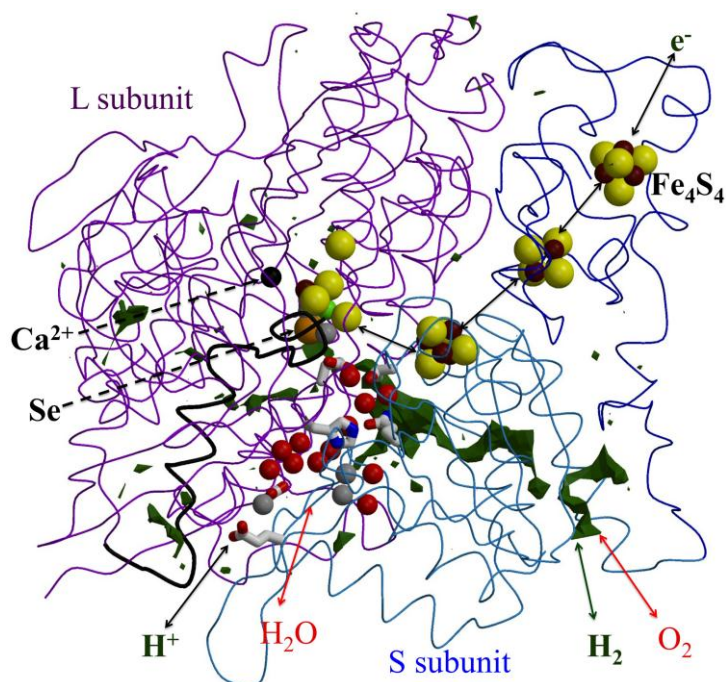


**Figure S2.** Protein fold and pathways in *Dmb* [NiFeSe]-hydrogenase. Red and grey spheres indicate fully and partially occupied water molecules, respectively, in hydrophilic tunnels. Other atom colors are the same as in Fig. 1-3. Hydrophobic cavities are indicated by a green surface.

**Calculations.** Hybrid quantum mechanical (QM) / molecular mechanical (MM) potentials in the QSite program from the Schrödinger Suite<sup>13</sup> were employed to investigate the conformation of the NiFeSe site and the residues in its vicinity, taking into account the effect of the protein matrix. The QM part consisted of the NiFe(CN)<sub>2</sub>CO site, the C $\alpha$  and side chain atoms of Cys70, Cys73, His77, Arg425, Se-Cys492 and Cys495 and, if present, Ni and Se-bound O-atoms and a water hydrogen-bonded to a seleninate. The LACVP\*\* basis set was used for metals, whereas the 6-31G\*\* basis set was applied to all other atoms treated quantum mechanically.<sup>14</sup> Density Functional Theory (DFT) with the M06 functional<sup>15</sup> was used for the QM part while the OPLS-2005 force field<sup>16</sup> was employed for the rest of the enzyme. Link atoms<sup>17</sup> were placed at the QM (C $\beta$ ) / MM (C $\alpha$ ) junction of Cys70, Cys73, His77, Arg425, Se-Cys492 and Cys495. Different protonation states of acidic and basic residues in the vicinity of the NiFeSe site were tested for selecting models closest to the crystallographically determined structures (Table S2). The results helped to determine reasonable distance restraints for crystallographic refinement of the active site and for excluding chemically unrealistic partial models.

**Table S2.** Superposition statistics for calculated QM/MM relative to refined X-ray model.

QM/MM vs <i>Nl</i> model state	9 Å sphere around Ni				QM-only region			
	Nat	$\Delta_{rms}$	$\Delta_{max}$	atom	Nat	$\Delta_{rms}$	$\Delta_{max}$	atom
Ox0 (Ni <sup>2+</sup> -OH <sub>2</sub> )	173	0.30	0.92	O <sub>513</sub>	36	0.20	0.34	Fe
Ox0 (Ni <sup>2+</sup> -OH <sup>-</sup> )	173	0.32	1.01	V <sub>23</sub> C $\gamma$ 2	36	0.22	0.48	C <sub>495</sub> S $\gamma$
Ox4b (Ni <sup>2+</sup> -O=Se-O <sup>-</sup> )	175	0.30	0.98	O <sub>513</sub>	38	0.18	0.42	O <sub>503</sub>

## References

- 1 M.C. Marques, R. Coelho, A.L. De Lacey, I.A.C. Pereira and P.M. Matias, *J. Mol. Biol.*, 2010, **396**, 893.
- 2 P.A. Karplus and K. Diederichs, *Science*, 2012, **336**, 1030.
- 3 W. Kabsch, *Acta Cryst. D*, 2010, **66**, 125.
- 4 M.D. Winn, C.C. Ballard, K.D. Cowtan, E.J. Dodson, P. Emsley, P.R. Evans, R.M. Keegan, E.B. Krissinel, A.G. Leslie, A. McCoy, S.J. McNicholas, G.N. Murshudov, N.S. Pannu, E.A. Potterton, H.R. Powell, R.J. Read, A. Vagin and K.S. Wilson, *Acta Cryst. D*, 2011, **67**, 235.

- 5 A.J. McCoy, R.W. Grosse-Kunstleve, P.D. Adams, M.D. Winn, L.C. Storoni and R.J. Read, *J. Appl. Cryst.*, 2007, **40**, 658.
- 6 E. Garcin, X. Vernede, E.C. Hatchikian, A. Volbeda, M. Frey and J.C. Fontecilla-Camps, *Structure*, 1999, **7**, 557.
- 7 P.Emsley, B. Lohkamp, W.G. Scott and K. Cowtan, *Acta Cryst. D*, 2010, **66**, 486.
- 8 G.N. Murshudov, P. Skubák, A.A. Lebedev, N.S. Pannu, R.A. Steiner, R.A. Nicholls, M.D. Winn, F. Long, and A.A. Vagin, *Acta Cryst. D*, 2011, **67**, 355.
- 9 R.J. Read, *Acta Cryst. A*, 1986, **42**, 140.
- 10 P.J. Kraulis, *J. Appl. Cryst.*, 1991, **24**, 946.
- 11 M.C. Lawrence and P. Bourke, *J. Appl. Cryst.*, 2000, **33**, 990.
- 12 E.A. Merritt and D.J. Bacon, *Meth. Enzymol.*, 1997, **277**, 505.
- 13 a) QSite version 5.6; b) Jaguar version 7.7 S, LLC, New York, NY, 2010.
- 14 P.J. Hay and W.R. Wadt, *J. Chem. Phys.*, 1985, **82**, 299.
- 15 Y. Zhao and D.G. Truhlar, *Theor. Chem. Acc.*, 2008, **120**, 215.
- 16 W.L. Jorgensen, D.S. Maxwell and J. Tirado-Rives J, *J. Am. Chem. Soc.*, 1996, 118, 11225.
- 17 P. Amara and M.J. Field, *Theor. Chem. Acc.*, 2003, **109**, 43.